Solvent Effects on the Dimerization Equilibria in Lennard-Jones Mixtures. Application of Wertheim's Theory of Association

A. Kovalenko,[†,‡] O. Pizio,*[,†] and D. Henderson[§,||]

Instituto de Química de la UNAM Circuito Exterior, Coyoacán 04510, México, D.F. México, Department of Chemistry and Biochemistry, Brigham Young University, Provo, Utah 84602, and Department of Chemical Engineering, Illinois Institute of Technology, Chicago, Illinois 60616

Received: October 25, 1996; In Final Form: February 21, 1997[⊗]

We consider a model of a two-component solution that consists of chemically reacting solutes and a chemically inert solvent. The particles interact via Lennard-Jones potentials. In addition, a directional associative interaction between the solute molecules promotes the formation of dimers. The theory for association in fluids of Wertheim is used to study the dimerization equilibrium. A multidensity Ornstein−Zernike equation is solved with the associative mean spherical approximation and, in some cases, with the hypernetted chain approximation. Some quantitative characteristics of dimerization in solution are obtained. We discuss the pair distribution functions, the solute−solvent coordination numbers, the partial molar volumes, and the compressibility, under varying conditions. Our particular concern is near-critical mixtures. The results, obtained with an explicit allowance for the chemical association between the reactants, show an enhanced solute−solvent clustering in near-critical solutions. The states distant from the critical region are characterized by more usual solvation of the solute molecules.

1. Introduction

The understanding of solvent effects on chemical reactions in condensed phases is a fundamental problem in physical chemistry. A very detailed discussion of the state of art of this research, in general and particularly for solutions important in organic chemistry, has been given in a monograph.[1] As it seems unnecessary to present arguments justifying the interest and importance of the study of this problem at a *microscopic* level using statistical mechanical tools, we would like to emphasize merely the diversity of the solvent influence on reactions in solutions, their crucial dependence on the interactions between species, and the thermodynamic state of the system. This latter aspect of the problem is one of the central issues of basic and applied studies of supercritical fluids.[2,3]

Several theoretical attempts to investigate supercritical solvents at a microscopic level and the problem of the influence of the solvent on the properties of solutions have been undertaken during last decade (see, e.g. refs 4−16). The method of integral equations for the theory of classical fluids has been used in some of these studies (see, e.g. refs 8−10,13−16). It seems to be an appropriate tool, because it possesses sufficient predictive power, and is at least qualitatively accurate for the calculation of structural and thermodynamic properties of solutions in a wide range of states, except very close to a critical point where the mean field behavior of the integral equation theories is qualitatively inconsistent with actual nonclassical behavior. Moreover, it is easier to investigate the region of low solute concentrations, as well as near-critical and supercritical solutions, by integral equations than by computer simulations. However, for the case where the interparticle interactions do not yield analytical solutions, very sophisticated numerical techniques are required to obtain numerical solutions close to the critical region.

Computer simulations for near-critical solutions are difficult. A set of methodological problems is encountered, either due to inadequate statistics prohibiting accurate averages or due to the very long-range fluctuations close to the critical region.[4−6] Generally, one must rely on the approximate but useful integral equation approach. However, it is impossible to discard the method of computer simulations, even for "delicate" states such as those near criticality, and emphasize only integral equations. Computer simulations permit a determination of the validity and accuracy of a particular integral equation approximation even near critical points. Such a verification has been performed[13] by a comparison of Monte Carlo and hypernetted chain (HNC) integral equation results. However, as may be seen from the lack of well-pronounced long-range asymptotics in the distribution functions that they report, the states are somewhat distant from the critical region.

In this study we focus on another related problem. In previous studies of near-critical mixtures, the effect of the aggregation of solutes and of solute−solvent clustering have been discussed extensively and profoundly[4−11] in order to find the relationship between theory and a wide set of experimental, mostly spectroscopic, results (see, e.g. refs 14−19). However, none of the previous theoretical studies have included explicitly the effect of chemical association. This we attempt here.

The problem of the influence of the solvent on chemical association in solutions can be studied successfully using the recent fundamental developments in the theory of chemical association in fluids by Wertheim[20−23] and by Stell et al.[24−28] This theoretical approach and a model of Cummings and Stell[29−31] have been developed and applied to solutions comprising a reacting component and a hard sphere and Yukawa solvent.[30,31] However, this method necessitates the adjustment of the theoretical approximation to satisfy the law of mass action. The theory of Wertheim[20−23] lacks this problem, but it is only recently[32,33] that it has been used to study solvent effects in solutions.

In this article, our primary goal is to construct and investigate a model solution consisting of solvent particles interacting via

[†] Instituto de Química de la UNAM Circuito Exterior.
[‡] Permanent address: Institute for Condensed Matter Physics, National Academy of Sciences of Ukraine, Lviv 11, Ukraine.
[§] Brigham Young University.
[||] Illinois Institute of Technology.
[⊗] Abstract published in *Advance ACS Abstracts,* April 1, 1997.

S1089-5647(96)03326-3 CCC: $14.00

Lennard-Jones (LJ) potentials and containing a chemically reacting (solute) component in which the particles, in addition to the LJ potential, interact via directional, finite-ranged forces. Association between the solute species, $A + A \rightleftharpoons A_2$, yields dimers in our model, similar to ref 22. We apply the theory of Wertheim[20−23] to study the dimerization equilibrium and its dependence on the parameters of the solvent model and on the thermodynamic state. In the explicit presence of chemical association, we calculate a wide set of properties of this model, which includes the pair distribution functions, the dimer fraction, the equilibrium association constants, the coordination numbers, the partial molar volumes of the reactants of the solvent species, as well as the compressibility of the model, in the range of parameters both distant and close to the region of solvent criticality. We apply different closure approximations to avoid the misinterpretation of possible anomalies as real results. Unfortunately, in the absence of a sufficient set of simulations for near-critical mixtures, which represents a difficult but important and urgent task on its own, we must restrict ourselves to a qualitative evaluation of the results. These are discussed in the context of the previous theoretical research on this subject and are compared, indirectly, with experimental observations.

2. A Model for the Chemically Reacting Lennard-Jones Mixture

The model for the solution is constructed in the following manner. We consider a two-component mixture consisting of reactants and solvents, which interact via the potentials

$$U_{ij}(1, 2) = U_{ij}^{\text{non}}(|\mathbf{r}_{12}|) + \delta_{ir}\delta_{jr}\, U_{\text{as}}(x_{12}) \tag{1}$$

where the subscripts i and j take values r and s, corresponding to the reacting solute particles and nonreacting solvent particles, respectively. The nonassociative terms for the solute−solvent (rs) and solvent−solvent(ss) interactions are taken in the form of Lennard-Jones (LJ) potentials:

$$U_{ij}^{\text{non}}(r_{12}) = 4\epsilon_{ij}\left[\left(\frac{\sigma_{ij}}{r_{12}}\right)^{12} - \left(\frac{\sigma_{ij}}{r_{12}}\right)^{6}\right] \tag{2}$$

The parameters ϵ_{ij} and σ_{ij} are the energies of interaction and the diameters of the Lennard-Jones particles. The dimensionless solute and solvent densities are denoted as ρ_r^* and ρ_s^*, $\rho_i^* = \rho_i\sigma_i^3$, respectively.

The solute−solute interaction potential, $U_{\text{rr}}(1,2)$, contains, in addition, the associative contribution $U_{\text{as}}(x_{12})$, which promotes the formation of the products of reaction between solutes. This is a simplified model solution. The associative interactions between the solvent species, as well as the associative solute−solvent interactions, can be included in the model also, depending on the actual physical situation.

We restrict our attention to the dimerization equilibria between solute species. Thus, we must choose an appropriate model for the dimerization. In this study, we consider a model in which dimerization occurs due to the directional associative interaction between square-well type attractive sites located inside the soft core of the solute particles. Each particle has one site that is displaced from its center. This model, with a hard core nonassociative interaction and attractive sites, has been proposed by Wertheim in ref 22. However, the model studied in ref 22 does not possess a liquid−gas phase transition and, in particular, does not permit the study of reactions in supercritical solvents. Therefore, the nonassociative interactions are taken as LJ potentials. The nonassociative interaction between solutes is

$$U_{\text{rr}}^{\text{non}}(r_{12}) = \begin{cases} \infty, & r_{12} < \text{L} \\ D, & L < r_{12} < 2d + a \\ 4\epsilon_{\text{rr}}\left[\left(\frac{\sigma_{\text{rr}}}{r_{12}}\right)^{12} - \left(\frac{\sigma_{\text{rr}}}{r_{12}}\right)^{6}\right], & r_{12} > 2d + a \end{cases} \tag{3}$$

The associative interaction is chosen similar to the Wertheim model:[22]

$$U_{\text{as}}(x_{12}) = \begin{cases} -\epsilon_{\text{as}} - D, & x_{12} < a \\ 0, & x_{12} > a \end{cases} \tag{4}$$

We have introduced the following notation: ϵ_{as} is the association energy, D is the height of the square mound (it is a large positive constant, which does not appear in the numerical solution as will be seen in below), $x_{12} = |r_{12} + \mathbf{d}(\Omega_1) - \mathbf{d}(\Omega_2)|$ is the distance between the sites on the particles 1 and 2; the displacement of the site in the particle i from its center and the orientation of the site are denoted as $\mathbf{d}$ ($|\mathbf{d}_i| = d$), and Ω_i, respectively. The width of the attractive well of the site−site interaction is a and, finally, L is the bonding distance. Similar to the case of a hard core,[22] we choose the geometric parameters of the associative interaction to satify the saturation condition at the dimer level, $L < 2d + a < L + (2 - 3^{1/2})d$. That is, no trimers or higher order n-mers can be formed with this value of L. Due to the stiffness of Lennard-Jones potential at small interparticle separations, we have replaced it by a hard core for $r < L$ in eq 3. We assume the Lorentz−Berthelot combination rules for the solute−solvent interaction parameters, i.e. ($\epsilon_{ij} = \epsilon_{ii}\epsilon_{jj})^{1/2}$ and $\sigma_{ij} = (\sigma_{ii} + \sigma_{jj})/2$.

To describe the dimerization of the solute molecules in the solvent, we use Wertheim's theory for association in fluids.[20−23] Let us consider the important ingredients that are necessary for our application. The Mayer function of the solute−solute interaction is represented in the form

$$f_{\text{rr}}(1,2) = \exp[-\beta U_{\text{rr}}(1,2)] - 1 = f_{\text{rr}}^{\text{non}}(r_{12}) + F_{\text{as}}(r_{12}) \tag{5}$$

where

$$f_{\text{rr}}^{\text{non}}(r_{12}) = \exp[-\beta U_{\text{rr}}^{\text{non}}(r_{12})] - 1 \tag{6}$$

and

$$F_{\text{as}}(r_{12}) = \exp[-\beta U_{\text{rr}}^{\text{non}}(r_{12})] \times \int \mathrm{d}\Omega_1\, \mathrm{d}\Omega_2\, \{\exp[-\beta U_{\text{as}}(1,2)] - 1\} \tag{7}$$

is the orientationally averaged associative Mayer function.[20−23] With sufficient accuracy it can be taken similarly to the original Wertheim model[22]

$$F_{\text{as}}(r) = \exp[\beta\epsilon_{\text{as}}]\frac{(2a - 2d + r)(a + 2d - r)^2}{24d^2 r} \tag{8}$$

for $L < r < 2d + a$; $F_{\text{as}}(r) = 0$, otherwise. The square mound, initially assumed in the region $L < r < 2d + a$, drops out from the numerical solution. The Mayer functions of the solvent−solvent and solute−solvent interactions are, as usual, the following:

$$f_{ij}(1,2) = f_{ij}^{\text{non}}(r_{12}) = \exp[-\beta U_{ij}^{\text{non}}(r_{12})] - 1 \tag{9}$$

Let us now proceed with the theoretical method.

3. Application of Wertheim's Theory for Association

To study this model we use a multidensity Ornstein−Zernike equation,[20,21] which reads

$$h_{ij}^{\alpha\beta}(r_{12}) - c_{ij}^{\alpha\beta}(r_{12}) = \sum_{\mu,\nu} \rho_r^{\mu\nu} \int d\mathbf{r}_3 \, c_{ir}^{\mu\nu}(r_{13}) \, h_{rj}^{\nu\beta}(r_{32}) + \rho_s^{00} \int d\mathbf{r}_3 \, c_{is}^{\alpha 0}(r_{13}) \, h_{sj}^{0\beta}(r_{32}) \quad (10)$$

where the matrix of densities for the solute subsystem has the form

$$\rho_r = \begin{pmatrix} \rho_r & \rho_r^0 \\ \rho_r^0 & 0 \end{pmatrix} \quad (11)$$

and $\rho_s^{00} = \rho_s$ is the solvent density. The matrix given by eq 11 has elements which correspond to the total density of reactant ρ_r and the density of undimerized reactants ρ_r^0. The *partial* pair correlation functions of Wertheim, $h_{ij}^{\alpha\beta}(r_{12})$, in eq 10 possess superscripts that correspond to the bonded or unbonded states of the particles; the superscripts 0 show that each of the particles 1 and 2 do not belong to dimers whereas the superscripts 1 correspond to the dimerized state of these particles. The partial correlation functions are related to the usual *total* pair correlation function (see, e.g. refs 22 and 34):

$$h_{rr}(r) = h_{rr}^{00}(r) + 2(\rho_r^0/\rho_r) h_{rr}^{01}(r) + (\rho_r^0/\rho_r)^2 h_{rr}^{11}(r) \quad (12)$$

The solute−solvent correlation functions are

$$h_{rs}(r) = h_{sr}(r) = h_{rs}^{00}(r_{12}) + (\rho_r^0/\rho_r) h_{rs}^{10}(r) \quad (13)$$

Finally, the solvent−solvent correlation function is $h_{ss}(r) = h_{ss}^{00}(r)$. The *partial* direct correlation functions $c_{ij}^{\alpha\beta}(r_{12})$ do not have a representation similar to eqs 12 and 13. However, for the solvent subsystem we have $c_{ss}^{00}(r) = c_{ss}(r)$.

The important element of Wertheim's approach for association is the self-consistency relation between the total and "bonded" densities.[20−23] In our case, the total density of species r and nonbonded fraction of reactants are related by

$$\rho_r = \rho_r^0 + (\rho_r^0)^2 \int d\mathbf{r} \, F_{as}(r) \, y_{rr}^{00}(r) \quad (14)$$

where $y_{ij}^{\alpha\beta}(r)$ is the *partial* cavity distribution function. The relation between *partial* correlation functions and cavity distribution functions is[20−23,34]

$$h_{rr}^{\alpha\beta}(r) + \delta_{\alpha 0}\delta_{\beta 0} = \exp[-\beta U_{rr}^{non}(r)] y_{rr}^{\alpha\beta}(r) + \delta_{\alpha 1}\delta_{\beta 1} \, y_{rr}^{00}(r) \, F_{as}(r) \quad (15)$$

$$h_{rs}^{\alpha 0}(r) + \delta_{\alpha 0} = \exp[-\beta U_{rs}^{non}(r)] y_{rs}^{\alpha 0}(r)$$

$$h_{ss}(r) = h_{ss}^{00}(r) = \exp[-\beta U_{ss}^{non}(r)] y_{ss}^{00}(r) - 1$$

In the absence of the long-range interparticle interactions it would be natural to use the associative Percus−Yevick (PY) approximation.[21,34] This approximation has been used with success for pure associating fluids, i.e. in the absence of a solvent.

However, for the Lennard-Jones model we have decided to use the associative MSA and HNC closures. Because of the Lennard-Jones potential, we must solve the integral equations numerically. Both these approximations are expected to work better than the PY closure because of the presence of long-range interactions. The MSA may yield unphysical pair distribution functions for fairly strong attractive interactions whereas the HNC lacks this deficiency, in close similarity to their counterparts in the theory of nonassociative fluids. In addition, the application of these closures to near-critical solutions has some peculiarities that are worth discussing.

Often, many approximations that are used to describe the liquid state fail in the region close to phase transitions. In particular, the disappearance of reliable solutions of the HNC approximation determines the termination line. This termination line of the HNC solutions does not correspond to the spinodal line but can serve as a rough indication of the closeness of the system to its critical region. This issue has been investigated in detail in ref 35. In particular, it has been shown that the HNC approximation provides a reasonable estimate of the vapor branch of the phase diagram for a nonassociating Lennard-Jones fluid. However, the liquid density branch is underestimated by the HNC closure. Thus, the HNC is expected to be applicable for states distant from the critical region; it has been shown[13] that the HNC results reproduce the Monte Carlo simulation data for these states reasonably well. We do not discuss the application of the *reference* HNC closure[36] because, in spite of its higher accuracy for the phase diagram of LJ fluids compared with the conventional HNC closure, it is unable to reproduce the upper part of this diagram.[37] Previously, Lee, Cummings, and Stell have documented carefully the region in which the hybrid PY-MSA fails to yield reliable solutions for a mixture of reacting hard spheres and a Yukawa solvent.[31]

At present, it is well-established that the MSA approximation and its extensions, such as the soft core MSA and hybrid MSA,[38] are among the most useful equations for the near-critical and supercritical solutions.[37,39] In this work, the approach of the system to the critical regime is monitored as follows. From the MSA, usually one finds that, for a given solvent density, the fluctuations in the system increase with decreasing temperature and the pair distribution functions (pdfs) (similarly to the PY approximation) become long-ranged and the compressibility tends to infinity. This serves as natural indication of approach to the states on the spinodal line. Near criticality, even for a very slightly lower temperature, the numerical algorithm of the MSA suddenly becomes unstable and reliable numerical solutions disappear.

The associative MSA closure presented here, appropriate for a soft core potential, is a generalization of the soft core MSA closure of Zerah and Hansen[38] for nonassociative Lennard-Jones fluids. First, all the interparticle nonassociative potentials $U_{ij}^{non}(r)$ are decomposed into the short-range $U_{ij,sh}^{non}(r)$ and long-range parts $U_{ij,lr}^{non}(r)$. We use the Weeks−Chandler−Andersen prescription[40] to divide the nonassociative potentials

$$U_{ij}^{non}(r) = U_{ij,sh}^{non}(r) + U_{ij,lr}^{non}(r) \quad (16)$$

where

$$U_{ij,sh}^{non}(r) = \begin{cases} U_{ij}^{non}(r) - \epsilon_{ij}, & r < r_{min}^{ij} \\ 0, & r > r_{min}^{ij} \end{cases} \quad (17)$$

and where

$$U_{ij,lr}^{non}(r) = \begin{cases} \epsilon_{ij}, & r < r_{min}^{ij} \\ U_{ij}^{non}(r), & r > r_{min}^{ij} \end{cases} \quad (18)$$

r_{min}^{ij} denotes the location of the minimum of the potential between the species i and j. Thus, the associative MSA

approximation reads

$$c_{rr}^{\alpha\beta}(r) = \{\exp[-\beta U_{rr,sh}^{non}(r)] - 1\} y_{rr}^{\alpha\beta}(r) + \delta_{\alpha 1}\delta_{\beta 1} F_{as}(r)\, y_{rr}^{00}(r) + -\delta_{\alpha 0}\delta_{\beta 0}\beta\, U_{rr,lr}^{non}(r) \quad (19)$$

$$c_{rs}^{\alpha 0}(r) = \{\exp[-\beta U_{rs,sh}^{non}(r)] - 1\} y_{rs}^{\alpha 0}(r) - \delta_{\alpha 0}\beta\, U_{rs,lr}^{non}(r)$$

$$c_{ss}^{00}(r) = \{\exp[-\beta U_{ss,sh}^{non}(r)] - 1\} y_{ss}^{00}(r) - \beta U_{ss,lr}^{non}(r)$$

where the *partial* cavity distribution functions are defined by eq 15.

In contrast to the MSA and the RHNC, the associative version of the HNC approximation does not require the decomposition of the nonassociative potentials of the Lennard-Jones type into two terms. The HNC closure reads

$$c_{ij}^{00}(r) = \exp[-\beta U_{ij}^{non}(r) + \gamma_{ij}^{00}(r)] - \gamma_{ij}^{00}(r) - 1 \quad (20)$$

$$c_{ij}^{01}(r) = \exp[-\beta U_{ij}^{non}(r) + \gamma_{ij}^{00}(r)]\gamma_{ij}^{01}(r) - \gamma_{ij}^{01}(r)$$

$$c_{rr}^{11}(r) = \exp[-\beta U_{rr}^{00}(r) + \gamma_{rr}^{00}(r)]\{(\gamma_{rr}^{01}(r))^2 + \gamma_{rr}^{11}(r)\} + F_{as}(r)\exp[\gamma_{rr}^{00}(r)] - \gamma_{rr}^{11}(r)$$

where $\gamma_{ij}^{\alpha\beta}(r) = h_{ij}^{\alpha\beta}(r) - c_{ij}^{\alpha\beta}(r)$; i and j take values r and s.

Equation 10, supplemented by eq 14 for densities and by the relevant closure relation, either eq 19 or eq 20, is solved numerically using the highly efficient algorithm of Labik et al.[41] This numerical procedure combines the Newton−Raphson technique and direct iteration to solve the set of nonlinear algebraic equations that are obtained from the consideration of the multidensity Ornstein−Zernike (OZ) equations on a grid. The correlation functions, as well as the interaction potentials, are truncated for $r > 40.96\sigma_s$, i.e. after 4096 points separated by a step $\Delta r = 0.01\sigma_s$. Similar to studies of nonassociating near-critical fluids, at a particular temperature the algorithm looses stability. However, for these states, in the case of the multidensity OZ equations with the HNC we were able to obtain higher compressibilities, $\rho kT\chi_T \approx 40$, in comparison with the PY termination line, $\rho kT\chi_T \approx 15$.[8−10] Even higher compressibilities can be obtained using a Picard direct iteration algorithm for similar values for the distance of truncation and a step $\Delta r = 0.01\sigma_s$, as mentioned by the referee of our work.

Although important, the determination of the pair distribution functions of the species is not the primary goal of our study. We are interested in chemical association between the reactants. Qualitatively, this can be described in terms of the fraction of dimerized species $\chi_r = 1 - (\rho_r^0/\rho_r)$ and the reduced equilibrium association constant, K/K_0, where $K = (\rho_r - \rho_r^0)/(\rho_r^0)^2$ and

$$K_0 = \int d\mathbf{r}\, F_{as}(r) \quad (21)$$

is the association constant for a pure reactant at infinite dilution. Also, it is of interest to describe the coordination of species qualitatively. Similar to previous studies of nonassociating near-critical mixtures in the framework of integral equation methods,[8−10] the coordination is given in terms of the fluctuation integrals

$$G_{ij}(r^*) = \rho_j^* \int d\mathbf{r}\, h_{ij}(r) \quad (22)$$

which correspond to the excess running coordination numbers of species; r^* is the "cut-off" parameter. The partial molar volume of species i, v_i, and the compressibility of the mixture χ_T can be obtained, using the Kirkwood−Buff fluctuation formulas, and are calculated from the relations[8−10]

$$v_i = [1 + \rho_j^*(G_{jj} - G_{ij})]/[\rho^* + \rho_i^*\rho_j^*(G_{jj} + G_{ii} - 2G_{ij})] \quad (23)$$

and

$$\rho^* kT\chi_T = \frac{[1 + \rho_j^* G_{jj} + \rho_i^* G_{ii} + \rho_i^*\rho_j^*(G_{jj}G_{ii} - G_{ij}^2)]}{[\rho^* + \rho_i^*\rho_j^*(G_{jj} + G_{ii} - 2G_{ij})]} \quad (24)$$

where i and j take values r and s, and $\rho^* = \rho_r^* + \rho_s^*$ is the total dimensionless density.

Next we proceed with the description of our results.

4. Results and Discussion

The model for the dimerization reaction studied here is characterized by the following values of parameters: $L = 0.73$, $d = 0.38$, $a = 0.06$. Thus, the condition for saturation at dimer level is satisfied. The association energy ϵ_{as} was chosen to obtain different degrees of dimerization of the Lennard-Jones solutes.

Let us comment also on the choice of the parameters for the *nonassociative* interactions and the densities of the species. For simplicity, at this initial stage of our investigation of solvent effects and of the application of the theory of Wertheim to this problem, we choose the diameters of the solutes and solvents to be equal, i.e. $\sigma_s = \sigma_r = \sigma$. Extension to the case of unequal diameters of solutes and solvents is not difficult technically but an evaluation of the accuracy of the approximations involved would become more complicated. This case will be studied separately with the simultaneous application of a wider repertoire of theoretical techniques.

To characterize the Lennard-Jones attraction between the species, we use the dimensionless solvent temperature $T^* = T_s^* = kT/\epsilon_{ss}$ and the ratio $\epsilon_{rr}/\epsilon_{ss}$. In the majority of the following discussion we will consider low solute concentrations, i.e. low packing fractions for the solute, $\eta_r = \pi\rho_r^*/6$, whereas the solvent packing fraction $\eta_s = \pi\rho_s^*/6$ is varied starting from low values to a highly packed solvent. A similar range of densities for solutes and solvent has been investigated in[8−10] and is of interest for the study of near-critical and supercritical solutions.

We begin the discussion of our results with the pdfs, obtained using the MSA approximation, for a mixture containing the solute at low packing fraction $\eta_r = 2 \times 10^{-4}$ for different temperatures. The MSA estimate for the critical parameters of LJ fluid is: $\rho_{cr}^* = 0.293$ ($\eta_{cr} = 0.153$), and $T_{cr}^* = 1.34$.[37] These values have been obtained from the analytical solution of the MSA for a LJ potential fitted by a sum of two Yukawa potentials via the *energy* route. It is known, however, that the MSA is not thermodynamically consistent (similar to the PY approximation), and therefore, the values for ρ_{cr}^* and T_{cr}^* from the compressibility route would differ. To overcome this difficulty one could to apply the *generalized* MSA (as has been mentioned in ref 37) which, by construction, will yield self-consistent structural and thermodynamic properties of a system. However, at this initial stage of the study of near-critical associating fluids, we restrict our attention to the usual MSA; the qualitative features of the behavior of the properties of a system in the region close to criticality are expected to be qualitatively similar in the MSA and GMSA.

Because of the differences between the critical points as determined by different thermodynamic routes and because we cannot reach the spinoidal exactly, we determine the critical point from the compressiblity route and take the line where we fail to obtain numerical solutions as the approximate spinodal.

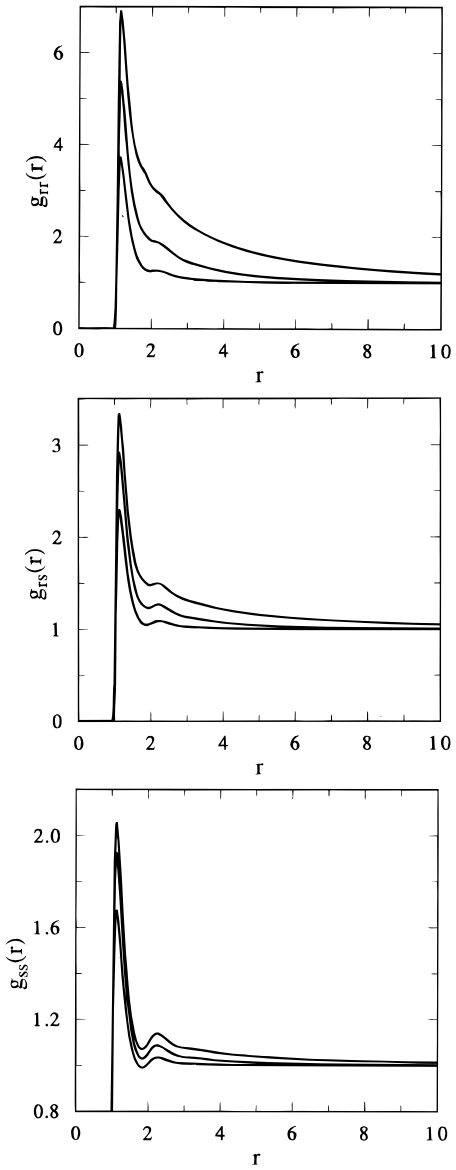

Figure 1. The pair distribution functions (associative MSA approximation) for a LJ mixture at $\eta_r = 2 \times 10^{-4}$, $\eta_s = 0.108$, $\epsilon_{as}/\epsilon_{rr} = 4.125$ for different temperatures, namely for $T^* = 1.0$, $T^* = 1.1$, and $T^* = 1.5$ from top to bottom. The solute−solute functions, $g_{rr}(r)$ are given in part a; the solute−solvent and solvent−solvent functions, $g_{rs}(r)$ and $g_{ss}(r)$, respectively, are given in parts b and c. The intermolecular part of $g_{rr}(r)$ is shown only.

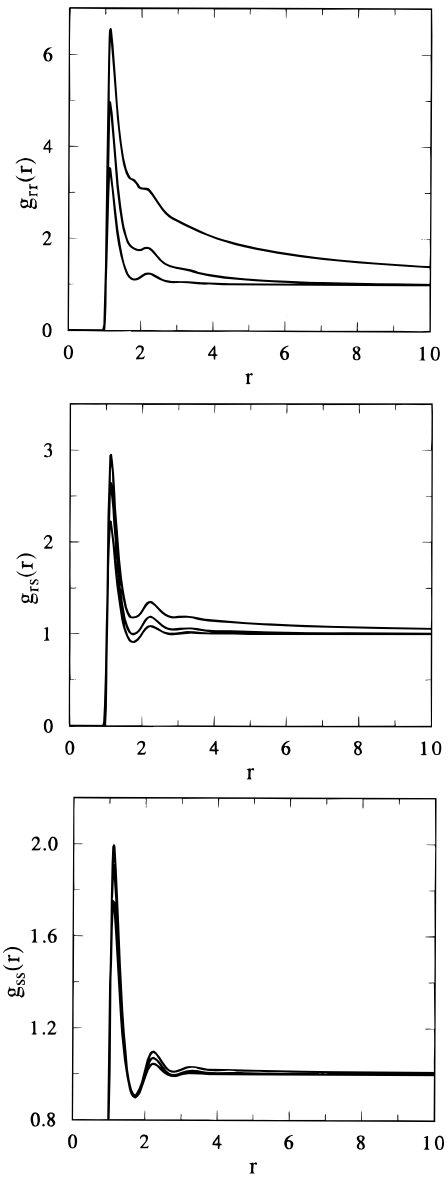

Figure 2. The same as in Figure 1 but at solvent packing fraction $\eta_s = 0.218$.

To emphasize uncertainties inherent in this procedure, we place the word critical in quotes.

The intermolecular parts of the pdfs, presented in Figures 1 and 2, are for the solvent density $\eta_s = 0.108$ and $\eta_s = 0.218$, respectively. Shortly, the intramolecular part of the solute−solute pdf will be discussed in terms of the dimer fraction. The curves shown in Figure 1 correspond to $\epsilon_{rr}/\epsilon_{ss} = 4.0$ and three values of the temperature, namely $T^* = 1.5$, $T^* = 1.1$, and $T^* = 1.0$; the association energy is chosen to be $\epsilon_{as}/\epsilon_{rr} = 4.125$. At the packing fraction $\eta_s = 0.108$, all the pdfs, $g_{ss}(r)$, $g_{rs}(r)$, and $g_{rr}(r)$, become increasingly long-ranged with decreasing temperature (Figure 1). For $T^* < 1.0$, we were unable to obtain reliable solutions for arbitrary solvent density. Thus, temperatures lower than $T^* = 1$ can be considered as "subcritical" temperatures in what follows. In fact, we will see that even $T^* = 1.0$ can be regarded as a "subcritical" temperature. Similar dependencies of the behavior of the pdfs on temperature are observed at $\eta_s = 0.218$ (Figure 2). However, the first maxima of all the pdfs are slightly higher for the case $\eta_s = 0.108$ than those for $\eta_s = 0.218$. At the higher density, we observe a more pronounced influence of the packing effects that, to some extent, supress the long-range tails of the pdfs. For both solvent densities, $\eta_s = 0.108$ and $\eta_s = 0.218$, the first maximum of the solute−solvent pdf is higher than that of the solvent−solvent pdf.

In Figure 3, we present the pdfs for the model at different solvent packing fractions and at $T^* = 1.076$. This is the lowest temperature at which we were able to obtain the solution of the MSA for an arbitrary solvent density. The solvent−solvent pdf, $g_{ss}(r)$, exhibts a long-range asymtotic behavior only at $\eta_s = 0.16$ ($\rho_s^* = 0.3055$), which is close to the "critical" density of the LJ fluid. For higher and lower solvent densities, the pdf tends to unity relatively quickly. There is a well-pronounced second maximum in $g_{ss}(r)$ for all three solvent densities in question, demonstrating short-range ordering effects. It can be seen from the solute−solvent pdf, $g_{rs}(r)$, that the solvation of a solute particle is largest at the solvent "critical" density. Further, it follows from Figure 3 that the solute particle is less coordinated, even for a more packed solvent, than at the "critical" density. Also, the solute−solute distribution function $g_{rr}(r)$ is long-ranged only at the "critical" solvent density. Moreover, the mutual coordination of solutes due to intermolecular correlations is the

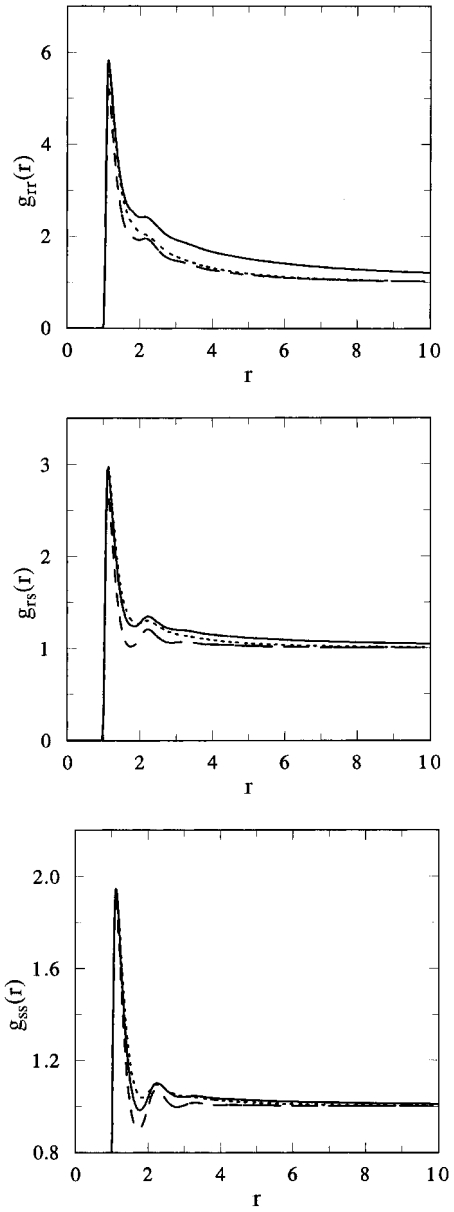

Figure 3. The pair distribution functions (associative MSA approximation) for a LJ mixture at $\eta_r = 2 \times 10^{-4}$, $\epsilon_{as}/\epsilon_{rr} = 4.125$, $T^* = 1.076$. The solvent−solvent, solute−solvent, and solute−solute functions are shown in parts a, b, and c, respectively. The dashed, solid, and dotted lines correspond to $\eta_s = 0.218$, 0.16, and 0.108, respectively.

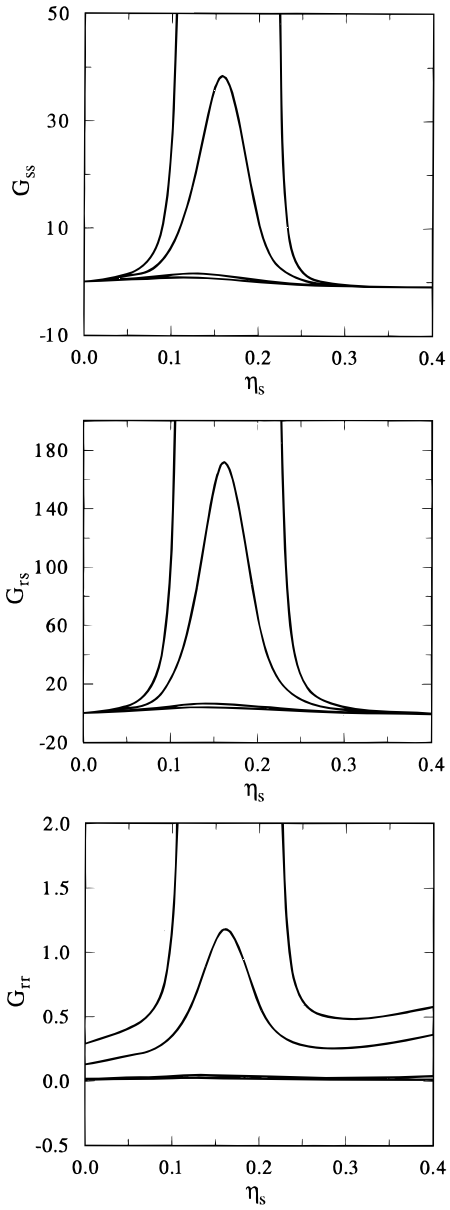

Figure 4. The dependence of fluctuation integrals (excess coordination numbers) $G_{ij}(r^* = 40)$ on the solvent packing fraction for the model defined in Figure 1 at different temperatures, namely for $T^* = 1.5$, $T^* = 1.35$, $T^* = 1.08$, and $T^* = 1.0$ from bottom to top. For the lowest temperature, $T^* = 1.0$, the divergency is observed. The G_{ss}, G_{rs}, and G_{rr} are presented in parts a, b, and c, respectively. The results are obtained in the MSA approximation.

weakest at $\eta_s = 0.218$ and strongest close to the "critical" density of the solvent.

To summarize the presentation of the pdfs, we conclude that at temperatures close to the termination line there is a much more preferable "clustering" of the solvent molecules around solute molecules than between the solvent molecules themselves, as seen in the long-range behavior of the solute−solvent and solvent−solvent pdfs near the termination line and the absence of this behavior for states distant from the termination line. Also, along the isotherm close to the maximum of the MSA termination line, the maximum solute−solvent coordination is observed at what we interpret to be the solvent "critical" density.

These trends can be discussed qualitatively in terms of the excess coordination numbers (fluctuation integrals), defined by eq 22. The fluctuation integrals $G_{ij}(r^*)$ are presented in Figure 4. We investigate the dependence of $G_{ij}(r^* = 40)$, that follows from the MSA, on the solvent packing fraction at different temperatures. Because the cut-off parameter is taken to be $r^* = 40$, we are considering a cumulative effect, rather than the local surroundings of a solute or solvent particle in terms of the solvation shells. It follows from the results shown in Figure 4 that for $T^* = 1.5$ and $T^* = 1.35$ the excess solute−solvent coordination number is large compared with the solvent−solvent value. However, the maximum value of G_{ss} and G_{rs} is observed in the region close to the "critical density" of the solvent. Thus, the solute−solvent "complexation" increases due to the increase of coordination between solvent particles. Also, the solute−solute coordination increases with solvent density but is much lower, as follows from Figure 4. It is interesting to mention that, for a highly packed solvent, approximately $\eta_s > 0.3$, the solute molecules try to pack closer. Only the region of solvent densities close to the critical density departs from the monotonous increase of G_{rr} with increasing η_s (Figure 4c).

For the "subcritical" temperature, $T^* = 1.0$, the excess coordination numbers diverge at two solvent densities, namely at $\eta_s \approx 0.11$ and at $\eta_s \approx 0.22$. While these two solvent densities

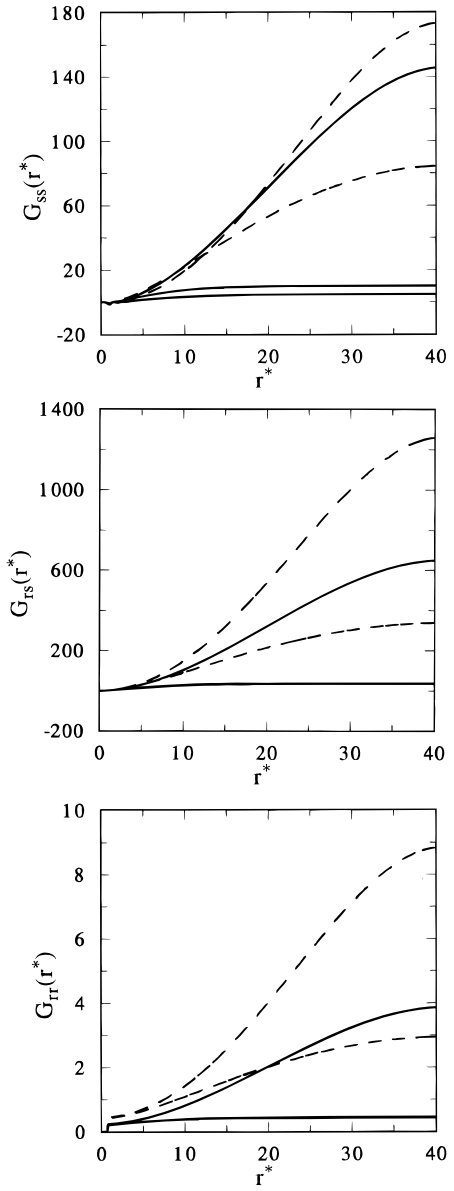

Figure 5. The dependence of the fluctuation integrals $G_{ij}(r^*)$ on the cut-off distance r^* at different solvent packing fractions for the model with $\eta_r = 2 \times 10^{-4}$, $\epsilon_{as}/\epsilon_{rr} = 4.125$, and $T^* = 1.0761$. The G_{ss}, G_{rs}, and G_{rr} from the MSA approximation are shown in parts a, b, and c, respectively. The solid curves from bottom to top in each part for $T^* = 1.076$ are for $\eta_s = 0.218$, $\eta_s = 0.108$, and $\eta_s = 0.16$; the dashed curves for subcritical temperature $T^* = 1.0$ from bottom to top are for $\eta_s = 0.108$ and for $\eta_s = 0.218$. In parts b and c, the results for $T^* = 1.0761$ coincide on the scale of the figure for solvent densities $\eta_s = 0.218$ and $\eta_s = 0.108$ and are shown by one curve.

are approached along the "subcritical" isotherm from below or from above, respectively, the solute−solvent coordination number is observed to be much larger than the solvent−solvent value. Thus, the enhanced solute−solvent clustering occurs not only for the solvent packing fraction close to the critical density but for all states close to the spinodal (we have in mind here the termination line of the MSA solutions which corresponds to the compressibility route). Although the properties of the system change in a continuous way along a "subcritical" isotherm, the effect of enhanced solute−solvent clustering is observed only in the vicinity of the solvent "critical" density.

The saturation of the excess cordination number occurs at large values of the cut-off parameter. Only for $r^* \approx 40$ at $\eta_s = 0.16$ do the functions $G_{ij}(r^*)$ tend to saturate at $T^* = 1.076$ (Figure 5). At this "critical" temperature, for lower and higher

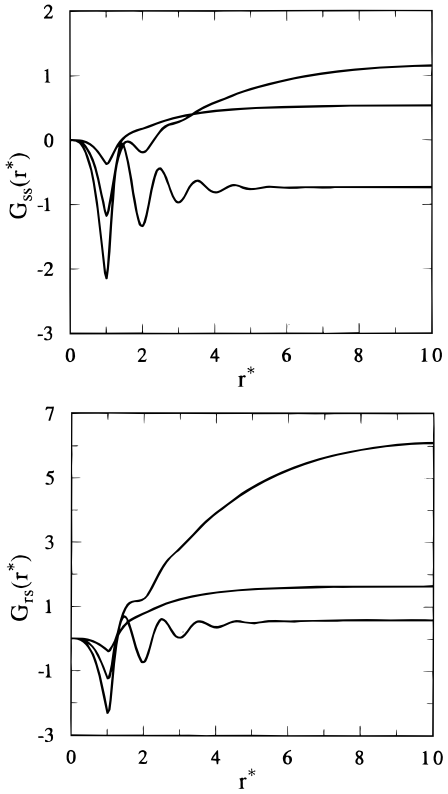

Figure 6. The dependence of the fluctuation integrals $G_{ij}(r^*)$ from the MSA approximation on the cut-off distance r^* at different solvent packing fractions for the model with $\eta_r = 10^{-8}$, $\epsilon_{as}/\epsilon_{rr} = 4.125$, and $T^* = 1.35$. The G_{ss} and G_{rs} are shown in parts a and b, respectively. The solid curves from bottom to top in each part are for $\eta_s = 0.3$, $\eta_s = 0.05$, and $\eta_s = 0.16$.

solvent densities that are distant from the "critical" value of density, the excess coordination numbers saturate at much lower distances, as expected. For a "subcritical" temperature, $T^* = 1.0$, we observe an anomalous increase of the coordination between solute and solvent molecules as well as between the solute molecules themselves on the termination line of the MSA solution. Saturation, as expected, is observed at large cut-off parameters. There is an essential difference between the coordination numbers on the gas and liquid branches of the termination line. Similar effects have been observed and discussed in terms of the equilibrium association constants by Lee, Cummings, and Stell.[31]

In Figure 6 we show the dependence of the saturation on the cut-off parameter for the excess solute−solvent and solvent−solvent coordination numbers for $\eta_r = 10^{-8}$ along a "supercritical" isotherm $T^* = 1.35$, distant from $T^* = 1.076$, at different solvent packing fractions. For this temperature, saturation already occurs at $r^* = 10$. However, the same tendency for the solute−solvent coordination number to increase at solvent densites close to the "critical density" is observed; however, this effect is much weaker than that at lower temperatures.

We now discuss the reduced equilibrium association constant K/K_0 and the fraction of dimerized reactants. The results of our calculations, using both the MSA and the HNC closures, are presented in Figure 7. We observe, for all the temperatures considered, that the MSA approximation yields the increasing values for $\ln(K/K_0)$ with increasing solvent packing fraction. For a higher temperature, $T^* = 1.5$, the curve behaves smoothly, whereas at lower temperature, $T^* = 1.35$, a shoulder on the curve develops at $\eta_s \approx 0.16$. A maximum value for $\ln(K/K_0)$ on the isotherm $T^* = 1.0761$ is observed at $\eta_s \approx 0.16$. This is

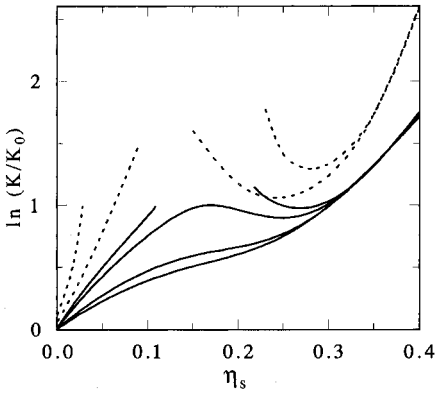

Figure 7. The dependence of the reduced equilibrium association constant K/K_0 on solvent packing fraction η_s. The results of the MSA and HNC approximation are shown by solid and dashed lines, respectively. The curves from bottom to top from the MSA theory (at $\eta_s = 0.1$) are for $T^* = 1.5$, $T^* = 1.35$, $T^* = 1.0761$, and $T^* = 1.0$; the HNC results from bottom to top (at $\eta_s = 0.25$) are for $T^* = 1.5$ and $T^* = 1.35$.

close to the solvent "critical" density. The MSA results for $\ln(K/K_0)$ are weakly sensitive on the solute concentration in the range $10^{-8} < \eta_r < 2 \times 10^{-4}$. For $T^* < 1.0761$ the MSA yields a discontinuity.

The behavior of the HNC results for $\ln(K/K_0)$ which are also given in Figure 7, shares some similarity with the MSA. However, there are differences. Even for $T^* = 1.5$, at $\eta_r = 2 \times 10^{-4}$, a region of solvent densities in which the HNC does not converge appears. This result is to be expected since the maximum of the HNC termination line for LJ fluid is substantially higher than that of the true critical temperature.[35] The most important qualitative conclusion that follows from these results is that both approximations, the MSA and HNC, show an enhanced reactivity of the solutes (increased $\ln(K/K_0)$ values) for the states close to their termination lines. The highest reactivity for "supercritical" isotherms occurs for the states close to the "critical" density of the solvent. In general, the MSA results are more reliable. However, the application of the schemes in the spirit of the generalized MSA are necessary to obtain consistency between the structural and thermodynamic properties of the states approaching critical region.

Very similar behavior of the results for the fraction of dimerized solutes, obtained from the MSA and HNC approximations, can be observed in Figure 8. An increase of the dimer fraction occurs as the spinodal point is approached. For "supercritical" isotherms, the maximum value for the dimer fraction is observed for the critical density of the solvent, as expected. For subcritical isotherms, we show only the case of $T^* = 1.0$. The difference in the fraction of dimers serves as an indication of the changes of the reactivity of solution in transition from the gas to liquid branch. Similar effects have been observed for reacting solutes in a Yukawa solvent but without solute−solvent attractive interactions.[31] It is of interest to examine the dependence of the dimer fraction on the association energy. For a higher association energy, $\epsilon_{as}/\epsilon_{rr} = 5.125$, the dimer fraction dependence on the solvent density is similar to the case $\epsilon_{as}/\epsilon_{rr} = 4.125$ but, in the former case, at the lower temperature nearly all reactants are dimerized. Augmenting the association energy yields a higher "critical" temperature. However, since we consider only a dilute solution, this effect is not very pronounced, at least for the energy parameters considered here.

The pdfs for the case $\epsilon_{as}/\epsilon_{rr} = 5.125$, with all other parameters held similar to the model studied at $\epsilon_{as}/\epsilon_{rr} = 4.125$, are shown in Figure 9. We have chosen $T^* = 1.08$ so that the region of

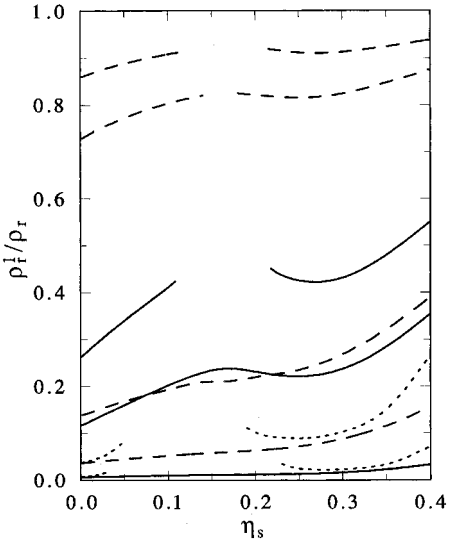

Figure 8. The MSA (solid and dashed lines) and HNC (dotted lines) dependence of the concentration of dimers χ_r on solvent packing fraction η_s for $\epsilon_{as}/\epsilon_{rr} = 4.125$ and $\epsilon_{as}/\epsilon_{rr} = 5.25$ at $\eta_r = 2 \times 10^{-4}$. The solid lines from bottom to top are for $T^* = 1.35$, $T^* = 1.0761$, and $T^* = 1.0$ ($\epsilon_{as}/\epsilon_{rr} = 4.125$). The dashed lines from bottom to top are for $T^* = 1.5$, $T^* = 1.35$, $T^* = 1.0761$, and $T^* = 1.0$ ($\epsilon_{as}/\epsilon_{rr} = 5.25$). The dotted lines from bottom to top are for $T^* = 1.35$ ($\epsilon_{as}/\epsilon_{rr} = 4.125$) and $T^* = 1.5$ ($\epsilon_{as}/\epsilon_{rr} = 5.25$).

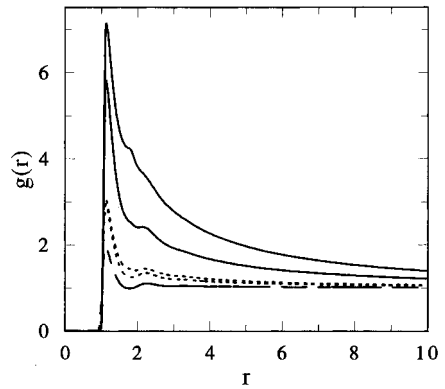

Figure 9. A comparison of the pdfs (MSA approximation here and in the following figures) for different association energies for the model with $\eta_r = 2 \times 10^{-4}$ and $\eta_s = 0.16$, $T^* = 1.08$. The $g_{rr}(r)$, $g_{rs}(r)$, and $g_{ss}(r)$ are given by solid, dotted, and dashed lines, respectively. The lower and upper curves, $g_{rr}(r)$ and $g_{rs}(r)$, are for $\epsilon_{as}/\epsilon_{rr} = 4.125$ and $\epsilon_{as}/\epsilon_{rr} = 5.125$, respectively. The $g_{ss}(r)$ curves coincide for both values of the association energy.

continuous solutions of the MSA remains for both association energies. The solvent−solvent pdf is almost unfluenced by the change of association energy. The solute−solvent and solute−solute functions are long-ranged. However, a higher value of association energy enhances their long-ranged behavior. The first maximum of $g_{rr}(r)$ increases as well as the values of this function for small separations, reflecting the enhanced mutual coordination of the solute particles.

As expected, the compressibility of the system becomes divergent on reaching the points on the MSA spinodal (Figure 10). The maximum compressibility is observed for the solvent "critical" density, whereas the solute partial molar volume v_r is minimal at this density (Figure 11). Usually the "near-critical" solutions are classified as attractive, weakly attractive, and repulsive, depending on the long-range enrichment or depletion of the solvent density around solute particles at solvent densities close to the "critical" density. The system under study belongs to the class of attractive "near-critical" solutions; the reactant partial molar volume is large and negative, diverging to $-\infty$ at

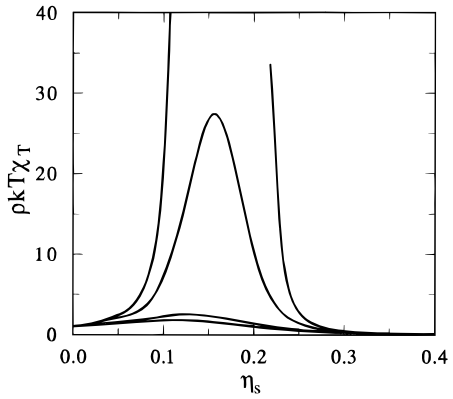

Figure 10. The dependence of the compressibility on solvent packing fraction for the isotherms $T^* = 1.5$, $T^* = 1.35$, $T^* = 1.0761$, and $T^* = 1.0$ (from bottom to top at $\eta_s = 0.1$), $\eta_r = 2 \times 10^{-4}$ and $\epsilon_{as}/\epsilon_{rr} = 4.125$.

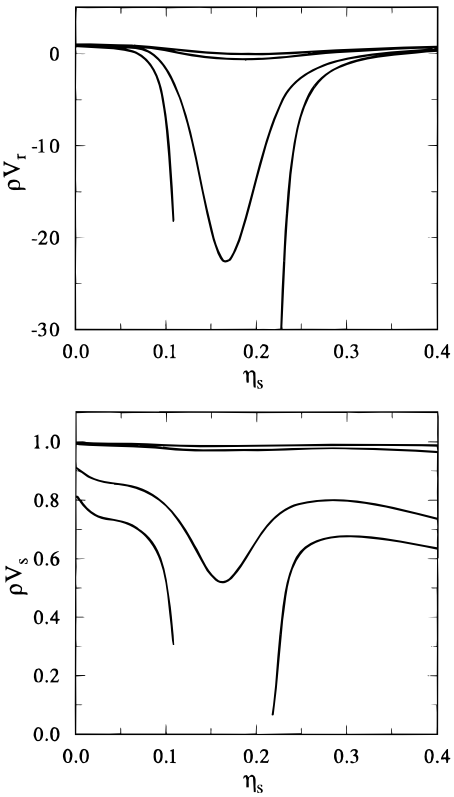

Figure 11. The dependence of the partial molar volumes of solute and solvent particles on solvent packing fraction (parts a and b, respectively) for the model as in Figure 10. The curves from top to bottom (at $\eta_s = 0.1$) are for $T^* = 1.5$, $T^* = 1.35$, $T^* = 1.0761$, and $T^* = 1.0$.

the "critical" point of the solvent. The behavior of the solvent partial molar volume v_s is presented in part b of Figure 11. The values of v_s are positive for a wide range of solvent density; in our model, only for "subcritical" isotherms does it change sign for solvent densities close to the "critical" density. The qualitative features of the behavior of thermodynamic properties of the model should be correct. However, we believe that the quantitative accuracy of these results can be improved by the application of more sophisticated models and closures.

5. Remarks

In this paper, associative versions of the common integral equations in the theory of fluids have been applied to study the problem of chemical reactions in supercritical and near-critical solvents. One difficulty with the approximations that we have considered is that the critical point is not well-defined. Different routes to thermodynamics lead to different "critical" points. Sometimes the "critical" point for one route lies inside the region for which no results can be obtained. This is annoying at very least. The generalized MSA approach forces the approximation to remove this problem. An associative generalized MSA is a potentially attractive technique but may not be a straightforward task. The RHNC approximation tends to be quite accurate. An associative RHNC approach should be explored. Other closures, such as the Verlet and its modifications could be considered. One of the best of the newer closures is the Duh−Hayment−Henderson closure[42,43] that has been found to be very accurate for Lennard-Jones fluid. It has not yet been tested in the critical region. Even so, an associative version of this approximation could be useful.

Another difficulty is that the termination line for the numerical solution of the equations is encountered before the spinodal. This is annoying in studies of the critical point. This problem seems to affect some approximations more than others. Whether this is a problem inherent in some approximations or merely a numerical artifact is not known.

Simulations of near-critical states of the model considered here, for both the associating and nonassociating case, are needed. Obviously, there is a limit on how close to the critical point one can go. Even so, such studies would be invaluable in testing the quantitative predictions of the approximations in the critical region.

When we are more confident of the accuracy of the approximations employed, more sophisticated models of association should be considered. For example, a chemically reactive solvent, which participates in the reaction between the solute molecules, might be considered. Cosolvents, such as CO_2 and CHF_3 can have a great effect on the properties of a near-critical and supercritical solution. Previous attempts to incorporate such effects into integral equations have not been very successful.

6. Acknowledgements A.K. is grateful to the program PEII of UNAM for financial support of this project. O.P. is grateful to M. C. Lozada García for stimulating discussions and continuous interest in the project. The interest and support of Professor D. Wasan is acknowledged. This work was supported in part by the National Science Foundation (Grants CTS 94-023584 and CHE96-01971) and Silicon Graphics Inc.−Cray Research of Mexico under University Research and Development Grant. We are grateful to the referee for valuable suggestions concerning this work.

References and Notes

(1) Reichard, C. *Solvents and Solvent Effects in Organic Chemistry*, 2nd ed.; VCH Verlagsgesellschaft: Weinheim, Germany, 1988.

(2) *Supercritical Fluid Science and Technology*; Johnston, K. P., Penninger, J. M. L., Eds.; ACS Symposium Series 406; American Chemical Society: Washington, DC, 1989.

(3) *Supercritical Fluid Extraction and Chromatography*; Charpentier, B. A., Sevenants, M. R., Eds.; ACS Symposium Series 366; American Chemical Society: Washington, DC, 1988.

(4) Petsche, I. B.; Debenedetti, P. G. *J. Chem. Phys.* **1989**, *91*, 7075.

(5) Petsche, I. B.; Debenedetti, P. G. *J. Phys. Chem.* **1991**, *95*, 386.

(6) Chialvo, A. A.; Debenedetti, P. G. *Ind. Eng. Chem. Res.* **1992**, *31*, 1391.

(7) Cummings, P. T.; Cochran, H. D.; Simonson, J. M.; Mesmer, R. E.; Karaboni, S. *J. Chem. Phys.* **1991**, *94*, 5606.

(8) Tom, J. W.; Debenedetti, P. G. *Ind. Eng. Chem. Res.* **1993**, *32*, 2118.

(9) Wu, R. S.; Lee, L. L.; Cochran, H. D. *Ind. Eng. Chem. Res.* **1990**, *29*, 977.

(10) Cochran, H. D.; Lee, L. L. In *Supercritical Fluid Science and Technology*; Johnston, K. P., Penninger, J. M. L., Eds.; ACS Symposium Series 406; American Chemical Society: Washington, DC, 1989; Chapter 3.
(11) Pfund, D. M.; Lee, L. L.; Cochran, H. D. *J. Chem. Phys.* **1991**, *94*, 3107.
(12) Pfund, D. M.; Lee, L. L.; Cochran, H. D. *J. Chem. Phys.* **1991**, *94*, 3114.
(13) Tanaka, H.; Shen, J. W.; Nakanishi, K.; Zeng, X. C. *Chem. Phys. Lett.* **1995**, *239*, 168.
(14) Kimura, Y.; Yoshimura, Y. *J. Chem. Phys.* **1992**, *96*, 3085.
(15) Kimura, Y.; Yoshimura, Y. *J. Chem. Phys.* **1992**, *96*, 3824.
(16) Kimura, Y.; Yoshimura, Y.; Nakahara, M. *J. Chem. Phys.* **1989**, *90*, 5679.
(17) Betts, T. A.; Zagrobelny, J.; Bright, F. V. *J. Am. Chem. Soc.* **1992**, *114*, 8163.
(18) Zagrobelny, J.; Bright, F. V. *J. Am. Chem. Soc.* **1992**, *114*, 7821.
(19) Zhang, J.; Lee, L. L.; Brennecke, J. F. *J. Phys. Chem.* **1995**, *99*, 9268.
(20) Wertheim, M. S. *J. Stat. Phys.* **1984**, *35*, 19, 35.
(21) Wertheim, M. S. *J. Stat. Phys.* **1986**, *42*, 459, 477.
(22) Wertheim, M. S. *J. Chem. Phys.* **1986**, *85*, 2929.
(23) Wertheim, M. S. *J. Chem. Phys.* **1987**, *87*, 7323.
(24) Stell, G.; Zhou, Y. *J. Chem. Phys.* **1989**, *91*, 3618.
(25) Zhou, Y.; Stell, G. *J. Chem. Phys.* **1992**, *96*, 1504, 1507.
(26) Zhou, Y.; Stell, G. *J. Chem. Phys.* **1995**, *102*, 7323.
(27) Stell, G. *Condens. Matter Phys.* **1993**, *2*, 4.
(28) Kalyuzhnyi, Yu.V.; Stell, G. *Mol. Phys.* **1993**, *78*, 1247.
(29) Cummings, P. T.; Stell, G. *Mol. Phys.* **1984**, *51*, 253.
(30) Cummings, P. T.; Stell, G. *Mol. Phys.* **1987**, *60*, 1315.
(31) Lee, S. H.; Cummings, P. T.; Stell, G. *Mol. Phys.* **1987**, *62*, 65.
(32) Kimura, Y.; Yoshimura, Y. *Mol. Phys.* **1992**, *76*, 737.
(33) Kovalenko, A.; Pizio, O.; Henderson, D.; Sokolowski, S. *Chem. Phys. Lett.* **1996**, *260*, 352.
(34) Kalyuzhnyi, Yu. V.; Stell, G.; Chapman, W. G.; Llano-Restrepo, M. L.; Holovko, M. F. *J. Chem. Phys.* **1994**, *101*, 7939.
(35) Ferreira, P. G.; Carvalho, R. L.; Telo de Gama, M. M.; Schlijper, A. G. *J. Chem. Phys.* **1994**, *101*, 594.
(36) Lado, F.; Foiles, S. M.; Ashcroft, N. W. *Phys. Rev. A* **1983**, *28*, 2374.
(37) Kalyuzhnyi, Yu. V.; Cummings, P. T. *Mol. Phys.* **1996**, *87*, 1459.
(38) Zerah, G.; Hansen, J. P. *J. Chem. Phys.* **1986**, *84*, 2336.
(39) Kalyuzhnyi, Yu. V.; Cummings, P. T. *Mol. Phys.* **1996**, *87*, 249.
(40) Weeks, J. D.; Chandler, D.; Andersen, H. C. *J. Chem. Phys.* **1971**, *54*, 5237.
(41) Labik, S.; Malijevsky, A.; Vonka, P. *Mol. Phys.* **1985**, *56*, 709.
(42) Duh, D.-M.; Haymet, A. D. J. *J. Chem. Phys.* **1995**, *103*, 2625.
(43) Duh, D.-M.; Henderson, D. *J. Chem. Phys.* **1996**, *104*, 6742.